

JOINT STATE-PARAMETER ESTIMATION IN A 3-D COUPLED PHYSICAL-ECOSYSTEM MODEL OF THE NORTH ATLANTIC: ASSIMILATION OF SEAWIFS DATA WITH A NON-GAUSSIAN EXTENSION OF AN ESRF

Ehouarn Simon and Laurent Bertino

Nansen Environmental and Remote Sensing Center, Bergen, Norway

Email: ehouarn.simon@nersc.no, laurent.bertino@nersc.no

ABSTRACT

We consider the application of an Ensemble Square Root Filter (ESRF) to a coupled ocean ecosystem model (HYCOM-NORWECOM). Such models, especially the ecosystem models, are characterized by strongly non-linear interactions active in ocean blooms and present important limitations for the use of data assimilation methods based on linear statistical analysis. Besides the non-linearity of the model, one is confronted with physical/biological constraints, the analysis state having to be consistent with the model, especially with the constraints of positiveness of some variables. Furthermore the non-Gaussian distributions of the biogeochemical variables break an important assumption of the linear analysis, leading to a loss of optimality of the filter. Finally ecosystem models and their coupling with physical ocean models present numerous uncertainties linked to the complexity of the processes that they aim at representing and the parameterizations that they introduce. Indeed these models are sensitive to numerous parameters that are poorly known.

We present an extension of the symmetric square root of the Ensemble Kalman filter (EnKF) dealing with these limitations by introducing a non-linear change of variables (anamorphosis function) in order to execute the analysis step in a Gaussian space. We also present the results of a joint state-parameter estimation in a North Atlantic configuration of the HYCOM-NORWECOM coupled model issued from the assimilation of SeaWiFS chlorophyll surface concentration data with this non-Gaussian extension of the ESRF.

Key words: non-Gaussianity, parameter estimation, anamorphosis, ecosystem model, SeaWiFS.

1. INTRODUCTION

The context of this work lies in the study and the forecast of the dynamics of the ocean and the evolution of its bi-

ology. The knowledge of the status of marine resources is too important to tolerate the risk of bad surprises. So analysis and short term forecasts of the primary production are needed by environmental agencies for monitoring algal blooms and possible movement of the fish populations [14]. In that effect, into the framework of the MyOcean¹ project, research activities attempt the reanalysis of the primary production and the biological components of the oceans, notably for the Arctic through the work package 5.

Such goals have led to the developments of numerical ecosystem models during the last decades, as well as their coupling with existing physical ocean models. Nevertheless these models present numerous uncertainties linked to the complexity of the processes that they try to represent and the parameterizations that they introduce. Even though many improvements have been made in the modelling of ocean ecosystems, the models are still too simple in comparison to the complexity of the ocean biology. In that effect, parameters remain poorly known and may vary in space and in time [15].

The main source of information lies in the observations of the ocean biology. Satellites allowed the community to obtain important informations on the biology. The observed surface ocean color provides informations on the distribution of the surface chlorophyll for a large area of the oceans, and thus the distribution of the phytoplankton. Satellite observations are also dependent on the atmospheric conditions, leading to loss of data of the ocean surface, especially for the Arctic ocean or the Nordic Seas with their frequent cloud cover. Finally, these satellite observations can present important errors, especially near the coast and are not able to provide information below the surface.

The interest of data assimilation methods is their ability to combine in an optimal way the heterogeneous and potentially erroneous information provided by the models and the observations. Nevertheless application of data assimilation methods to ecosystem models in an efficient way is a theoretically and practically challenging issue.

¹<http://www.myocean.eu.org>

On the one hand, the strongly nonlinear behavior of ecosystem models (especially during the period of the spring bloom) raises the question of which stochastic model to be used [3]. On the other hand one is also confronted with the model constraints: the analysis state has to be consistent with the model, especially under the constraints of positiveness of some variables. Most variables of ecosystem models are concentrations of a biological tracer, and cannot be negative. Finally the non-Gaussian distributions of most biogeochemical variables break an important assumption of the linear analysis, leading to a loss of optimality of the EnKF (and other linear filters). The optimality of the linear statistical analysis is proved under some assumptions, notably an assumption of Gaussianity made on the distribution of the variables (of the model and the observations) and the errors. In a previous study [17], we pointed out the ability and highlighted potentialities of a non-Gaussian extension of the EnKF for model state estimation in a context of twin experiments. The present study extends these previous works to the assimilation of real satellite observations for combined state-parameter estimation in an inevitably biased ecosystem model.

The outline of the paper is as follows. We present a deterministic square root of the EnKF with Gaussian anamorphosis in Section 2. We describe our experimental framework in Section 3. Results of the methods are discussed in Section 4, and we present our conclusions in Section 5.

2. A DETERMINISTIC SQUARE ROOT OF THE ENSEMBLE KALMAN FILTER WITH GAUSSIAN ANAMORPHOSIS

In the same way that the EnKF with Gaussian anamorphosis suggested by [3], this algorithm is based on the skeleton of the symmetric square root of the EnKF presented in [9] and divides into two steps:

Forecast : the forecast step is a propagation step in the EnKF that uses a Monte-Carlo sampling to approximate the forecast density by N realizations:

$$\forall i = 1 : N, \quad \mathbf{x}_n^{f,i} = f_{n-1}(\mathbf{x}_{n-1}^{a,i}, \epsilon_n^{m,i}) \quad (1)$$

with \mathbf{x}_n the state vector at time t_n , f_{n-1} the nonlinear model and ϵ_n^m the model error.

Analysis: the analysis step conditions each forecast member to the new observation \mathbf{y}_n by a linear update. The anamorphosis functions are introduced in this step.

For each variable of the model, at time t_n , we apply a function ψ_n which is a nonlinear bijective function from the physical space to a Gaussian space. We transform each variable separately. In order to simplify the notations, we consider the monivariate case (so one function

ψ_n). It reads:

$$\forall i = 1 : N, \quad \tilde{\mathbf{x}}_n^{f,i} = \psi_n(\mathbf{x}_n^{f,i}) \quad (2)$$

In practice, it means that we apply the changes of variable for each variable in every point of the discretized domain.

In the same way, we introduce an anamorphosis function χ_n for the observations \mathbf{y}_n at time t_n :

$$\tilde{\mathbf{y}}_n = \chi_n(\mathbf{y}_n). \quad (3)$$

The observation operator \mathbf{H} links the physical variables and the observations. We define the observation operator $\tilde{\mathbf{H}}_n$ linking the transformed variables and observations by the formula

$$\tilde{\mathbf{H}}_n = \chi_n \circ \mathbf{H} \circ \psi_n^{-1} \quad (4)$$

where \circ defines the function composition.

The linear analysis is realized on the transformed variables and observations according to the equations for the updates of the mean and the ensemble perturbations of the symmetric square root of the EnKF described in [9]. It requires the use of the transformed observation operator $\tilde{\mathbf{H}}_n$. The transformed Kalman gain matrix is built on the forecast error covariance matrix $\tilde{\mathbf{C}}_n^f$ approximated by the covariance of $(\tilde{\mathbf{x}}_n^{f,i})_{i=1:N}$.

The pull-back to the physical space is realized by using the inverse of the anamorphosis function:

$$\forall i = 1 : N, \quad \mathbf{x}_n^{a,i} = \psi_n^{-1}(\tilde{\mathbf{x}}_n^{a,i}) \quad (5)$$

The analyzed mean \mathbf{x}_n^a and the covariance matrix \mathbf{C}_n^a are approximated by the ensemble average and covariance of $(\mathbf{x}_n^{a,i})_{i=1:N}$.

3. DESCRIPTION OF THE EXPERIMENTAL FRAMEWORK

3.1. The coupled ocean ecosystem model

The experiments were performed in a North Atlantic and Arctic configuration of the HYCOM-NORWECOM coupled model. We describe briefly this configuration, which corresponds to the one in [17] and the coarse resolution one in [12].

The domain of the model covers the North Atlantic and the Arctic oceans north of 30°S. The grid was created using the conformal mapping algorithm outlined in [2].

The physical model used is the HYbrid Coordinate Ocean Model, HYCOM, [5]. The vertical coordinates are isopycnal in the open, stratified ocean, and change to z-level coordinates in the mixed layer and/or unstratified seas.

Table 1. Biological parameters to be estimated.

Parameter	Original value
Diatom temperature dependent P_{max}	0.063 ($^{\circ}C^{-1}$)
Flagellate temperature dependent P_{max}	0.063($^{\circ}C^{-1}$)
Metabolic loss rate temp. dependence	0.07 ($^{\circ}C^{-1}$)
Death rate	$1.6e^{-6}(s^{-1})$
Rate of decomposition detritus	$1.52e^{-7}(s^{-1})$
Extinction due to water and non chlorophyll	$0.07(m^{-1})$
Chlorophyll-a extinction coefficient	$1.38e^{-2}(mmgCHLa^{-1})$

The model uses 23 layers with a minimum thickness of 3m at the top layer. The model presents 216×144 horizontal grid points which corresponds to a horizontal resolution of 50 km. This is sufficient to broadly resolve the large-scale circulation.

The evolution of the ice cover in the Northern part of the domain (mainly in the Arctic Ocean) is taken into account by an on-line coupling between the physical ocean model and an ice module including a thermodynamic model [6] and a dynamic model (using the elastic-viscous-plastic rheology of [13]). Finally the ERA40 synoptic fields and climatological river runoff (excluding nutrients) are used to force the model.

The ecosystem model is the NORWegian ECOlogical Model system, NORWECOM, ([18], [1]). This model includes two classes of phytoplanktons (diatoms and flagellates), several classes of nutrients, and includes oxygen, detritus, inorganic suspended particulate matter (ISPM) and yellow substances classes. Nevertheless in our experiments ISPM and yellow substances were not activated. The ecosystem state vector is made up of 7 variables.

3.2. Data assimilation experiments

We focus on data assimilation in the ecosystem model. The multivariate assimilation of both physical and biological states is a challenging work and remains an open issue. According to [8, 9], the combined state-parameter estimation is realized by augmenting the state vector with the unknown parameters that one wants to estimate. Into practice, the state vector corresponds to the ecosystem state vector only, namely seven 3D variables, augmented by seven 2D biological parameters (see Table 1). Due to the lack of feedback in the coupling from the ecosystem model to the physical one, the assimilation does not correct the ocean physical state. Furthermore, the correction is realized in the first twelve upper layers (water between 0m and 600m) of the model only, to avoid the effect of spurious corrections in the bottom layers.

The assimilated observations are the 8-days Globcolour²

²<http://www.globcolour.info>

surface chlorophyll-a mapped products (case 1 water). The daily chlorophyll-a concentration is computed from the data obtained with different instruments (MERIS, MODIS and SeaWiFS). For our assimilating period (1998-1999), only SeaWiFS valid pixels contributed to the bin value. The 8-days products are then computed as the arithmetic mean of the daily merged data. We refer to [10] for a description of these products. It has to be pointed that the errors on surface chlorophyll provided from SeaWiFS chlorophyll data are on average of the order of 30% of the value ([11]), with important variations depending on the area. The resolution of the observations being 0.25° , that is higher than the resolution of the model, super-observations are generated by averaging the observation values on the model grid. These super-observations will be called observations in the following.

The observation error in the transformed space has a Gaussian distribution with a mean of zero and a standard deviation of 0.3: $\epsilon^o \sim \mathcal{N}(0, \sigma = 0.3)$. The anamorphosis functions being designed to generate transformed variables with a Normal distribution, the observation error in the transformed space is supposed to be around 30% of the transformed observation. Nevertheless, we introduce a warm up of the assimilation system by decreasing the values of the variance of the observation error σ from 1 (error of 100%) to 0.3 during the first months of the experiments: σ is equal to 1. during the first two months, then 0.6 during two additional months, and then 0.3.

At an observation point, \mathbf{H} relates linearly the chlorophyll-a concentration CHLA to the model diatoms and flagellates concentrations (DIA and FLA) by the equation (6).

$$CHLA = \frac{DIA + FLA}{11}. \quad (6)$$

The initial ensemble as from 20 November 1998 is made of 100 members obtained by running the model from 20 November 1997 with perturbations of the atmospheric fields in the physical model only (as done in [16]) and perturbed parameters. The perturbations induced in the physics by the atmospheric forcing then cascade in the ecosystem component of the coupled model. As the state vector is made of the biological component only, the assimilation cannot correct the errors induced by the perturbations in the physical component of the coupled model. In the final reanalysis and operational forecast products, a first step will consist in correcting the errors in the physical component by assimilating physical data, as already done in the TOPAZ operational forecast and monitoring system [4], and then the assimilation of chlorophyll-a satellite data will be done in the ecosystem component of the coupled model. Direct perturbations of the ecosystem component can also be added. This strategy may appear simplistic, nevertheless the biological module is still too uncertain to be used to correct the physics.

The initialization of the parameter ensemble is realized as from 20 November 1997 assuming that the parameters

are lognormal distributed and inhomogeneous in space around the original value specified in NORWECOM (see Table 1). The initial perturbed parameter p reads

$$p = p_0 \times e^{(Z - \sigma^2/2)} \quad (7)$$

with p_0 the NORWECOM value and $Z \sim \mathcal{N}(0, \sigma = 0.3)$ and the term in $\sigma^2/2$ is a bias correction. The parameters are constant during the forecast steps of the filter. It means that the evolution of the parameters is driven by the analysis steps only.

The random perturbations are generated by a spectral method [7] in which the horizontal variability is simulated using a spatial decorrelation radius of 250 km. The decorrelation time-scale is of five days. The standard deviations of the fields perturbed are: 0.03 N.m^{-2} for the eastward and northward drag coefficient, $\sqrt{2.5} \text{ m.s}^{-1}$ for the wind speed, $\sqrt{0.005} \text{ W.m}^{-2}$ for the radiative fluxes and 3° Celsius for the air temperature. These values correspond to the ones used in the TOPAZ operational forecast and monitoring system and in the twin experiments in [17].

Finally the assimilation system uses localization as suggested by [7]. The radius is constant and equal to 500km (10 cell-grids in the two horizontal directions). We have not introduced advanced implementation details as the decrease of the radius close to the coast for example in order to have a better understanding of the benefits of anamorphosis functions.

Meanwhile, a free-running simulation (called control run) has been conducted. It consists of a deterministic simulation without perturbation of the atmospheric fields, without data assimilation and with the nominal NORWECOM parameters.

3.3. Construction of the monivariate anamorphosis functions

Details of the construction of the monivariate anamorphosis functions are given in [17]. We highlight briefly the slight changes that were induced by passing from simulated to real observations.

We assume that each variable and the chlorophyll-a at different locations in space are identically distributed in a time period of three months centered on the datum of the analysis step. In that way we obtain time evolving anamorphosis functions. The choice of three months is motivated by the time scale of a typical bloom which lasts for about four months. Such a moving window allows for errors in the timing of the bloom to be included in the probability distribution function.

The experimental anamorphosis functions are computed from weekly output from a six year integration of the model. The anamorphosis function is piecewise linear,

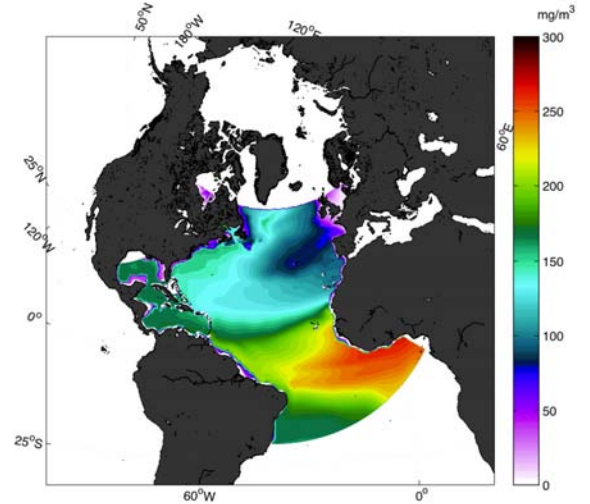


Figure 1. Inorganic nitrogen: example of spatial distribution of the data set used to build the empirical anamorphosis function during winter.

using linear interpolation of the experimental anamorphosis function. The middle of steps are used to interpolate the empirical anamorphosis functions, with the exception of the last right step for which the maximal value of the data set is used.

Due to model bias, data from ten years of satellite surface chlorophyll-a observations are include in the model data set to build the empirical anamorphosis function (Equation 3). It remedies the problem linked to observations out of the range of pure model data set and reduces the shift of the mean to high values.

Finally, an horizontal spatial localization is introduced in the construction of the empirical anamorphosis function. In order to follow the evolution of the spatial coverage of the observations, only data located south of a latitude defined from the highest latitude of observations are used. As we perform local analysis, the idea is to avoid to build the anamorphosis functions from data located out of observed areas. For example, we do not use data located in the Arctic ocean during winter as no observations are present in this area at that period, as illustrated in Figure 1.

4. RESULTS

4.1. Overall evolution of the errors

We follow the evolution in time of the Root Mean Square error (RMS) and the ensemble standard deviations (STD) of the solution of the assimilating system. The expression

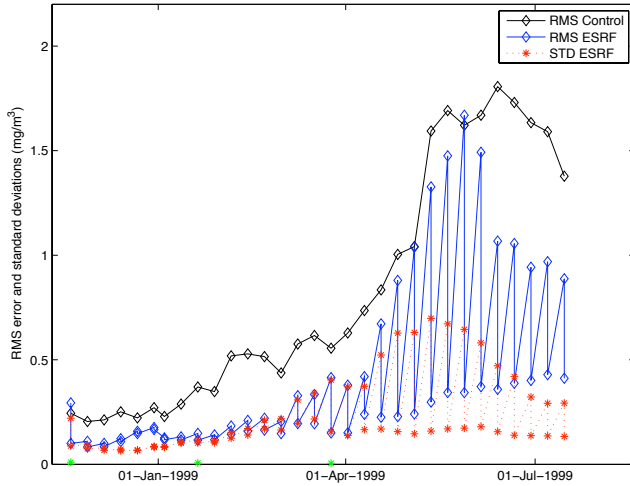


Figure 2. Surface chlorophyll-a: one year evolution of the RMS error and the standard deviations (mg/m^3). The green stars show the datum of change in the specification of the observation error in the filter (100%, 60% and 30%).

at time t_n of these two quantities is as follows:

$$\text{RMS}(t_n) = \sqrt{\frac{1}{\#\Omega} \sum_{\mathbf{k} \in \Omega} (\mathbf{y}(t_n, \mathbf{k}) - \mathbf{H}\bar{\mathbf{x}}(t_n, \mathbf{k}))^2}$$

$$\text{STD}(t_n) = \sqrt{\frac{1}{N-1} \frac{1}{\#\Omega} \sum_{\mathbf{k} \in \Omega} \sum_{m=1}^N (\mathbf{H}\mathbf{x}^m(t_n, \mathbf{k}) - \mathbf{H}\bar{\mathbf{x}}(t_n, \mathbf{k}))^2} \quad (8)$$

with Ω the domain of computation, $\#\Omega$ the number of grid points of the domain used for the computation of the RMS and STD, N the number of members, \mathbf{x}^t the true state, and $\bar{\mathbf{x}}$ the mean of the ensemble.

Figure 2 represents the evolution of the RMS error and the standard deviations over eight months for the surface chlorophyll-a (what we observe). In that case Ω is the top layer of the model. The black curve represents the evolution of the RMS error of the solution obtained by the control run.

First, we note that the system significantly reduces the error during the low productivity period. The standard deviation is in agreement with the RMS error, pointing out a relevant representation of the error by the ensemble, except for December 1998. During that initial month, the model bias is responsible for an irrelevant representation of the error. Furthermore, we note a drift of the ensemble from the biased climatology used to build the anamorphosis function, leading to non-Gaussian transformed variables and a locally irrelevant analyzed solution.

From March onwards, the RMS error and standard deviation significantly increase during the forecast steps, but remain in agreement with each other. After April when the bloom is starting, the assimilation system does not produce accurate 8-days forecasts. The RMS error

increases by a factor 5 during two analysis and almost reaches the RMS error of the control run during that period. We note also a large underestimation of the error by the filter during the bloom, betraying strong biases of the model.

4.2. Regional distribution of the errors

We examine the spatial localization of the error on the surface chlorophyll-a during the bloom. Figure 3 represents the maps of the mean innovation $\mathbf{H}\bar{\mathbf{x}}^f - \mathbf{y}$ on 4th May 1999.

We note that the natural trend of the model is to overproduce phytoplankton. The assimilation leads to a significant reduction of the forecast error in the Sargasso Sea where observations are present all year long. The combined state-parameter estimation in this area during the cold period leads to an ensemble that can handle the spring bloom. On the other hand, we note larger errors in the sub-Arctic gyre and in the Nordic Seas where no observations were available for assimilation before March. It is interesting to see that the combination of the advection of errors during the cold period preceding the bloom and perturbed parameters leads to a solution with a larger error than in the control run. The lack of satellite observations in the Arctic Ocean and the North Sea during winter is a major issue for the estimation of biased parameters in this area.

4.3. Local evolution of parameters

We are interested in the evolution with time of the mean and standard deviations of several parameters. These quantities are computed for one grid point in the Sargasso Sea (Figure 4) where observations are present all year long and in the North Sea (Figure 5) where no observations are present in winter.

First we note that the estimate of a parameter can drastically change with the spatio-temporal localization. So, according to the equation of the model, the too low concentration of phytoplankton in winter, for both regions leads to a decrease of the production rate temperature dependence (a2) in "warm" water (Sargasso Sea) and an increase in cold water (North Sea).

In the Sargasso Sea, the parameter a2 converges towards a low value despite the too large concentration of phytoplankton during the bloom. This overproduction of phytoplankton leads to a large delayed increase of the death rate parameter (cc3). The evolution of the decomposition rate detritus parameter (cc4) is more significant after April. Part of these delays might be explained by the overestimation of the observation error until end of March (warm-up). The values reached at the end of the experiments for a2 and cc3 being close to the minimal and maximal bounds specified in the definition of the

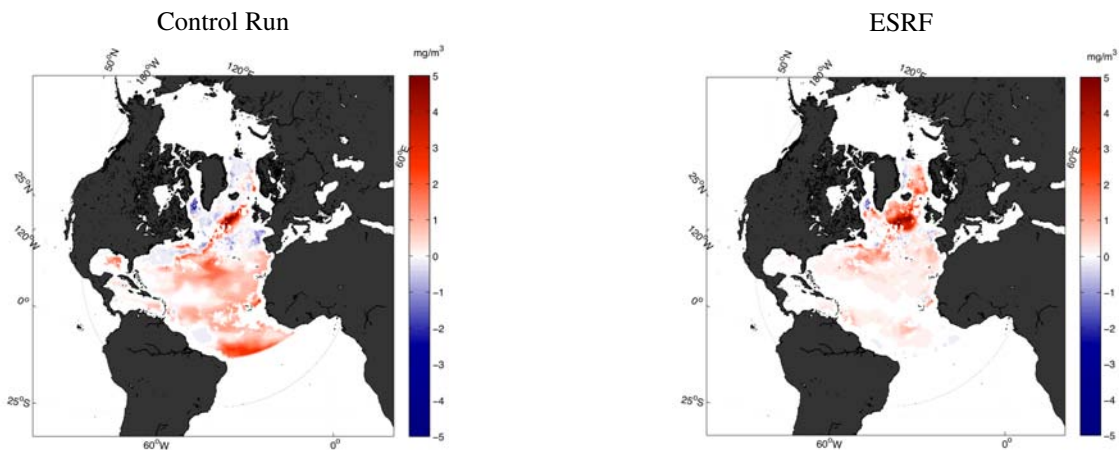


Figure 3. Chlorophyll-a forecast on 4 May: $\mathbf{H}\bar{\mathbf{x}}^f - \mathbf{y}$.

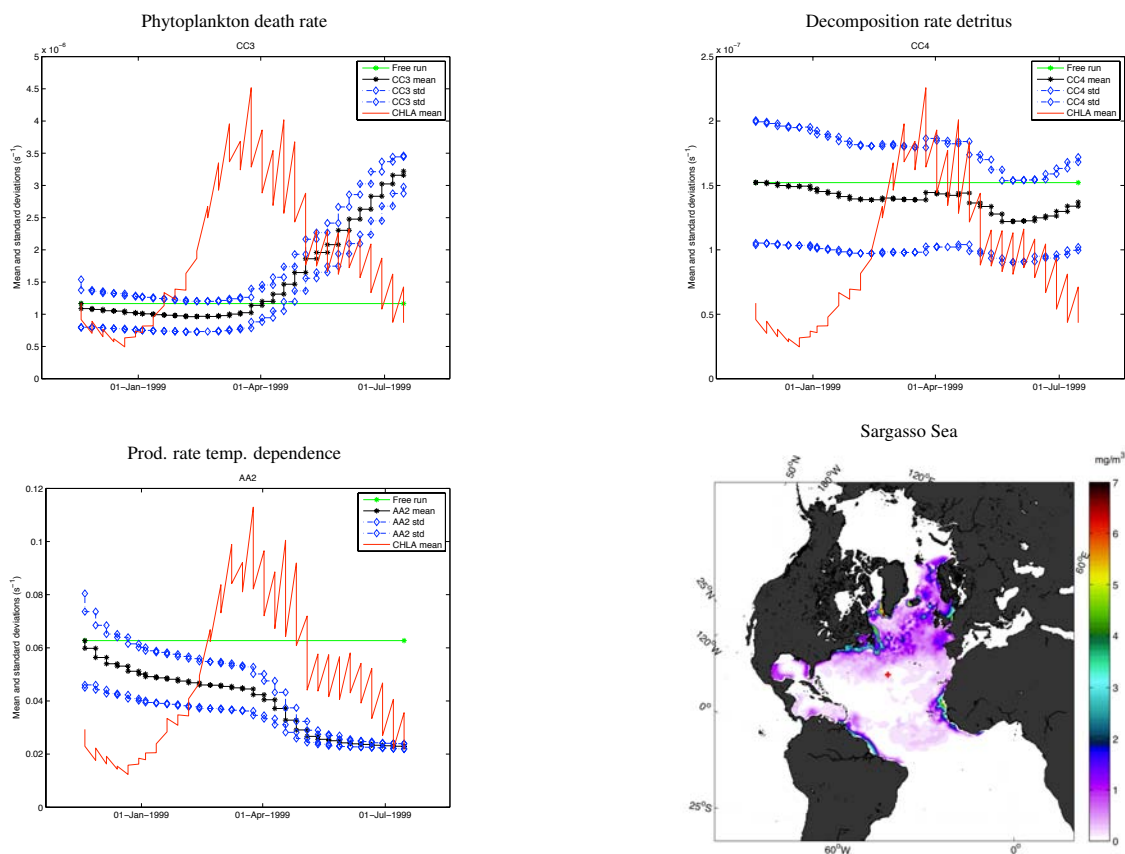


Figure 4. Evolution of local parameters in the Sargasso Sea. The grid point is localized with a red cross. The black line represents the evolution of the mean of the ensemble parameter. The blue lines represent the evolution of the mean plus/minus the standard deviation. The green line represents the original value of parameters in NORWECOM. The red curve represents the evolution of chlorophyll-a with time.

anamorphosis functions, it raises the question of the pertinence of such estimates.

In the North Sea, the lack of observations in winter does not allow the estimation of parameters before March. The too low concentration of phytoplankton in March leads to a large decrease of cc3 and slight increases of a2 and cc4. At the end of April, cc3 has almost converged towards a low value. Being "trapped" in this winter mode, corrections on this parameter cannot handle the too large bloom concentrations of phytoplankton. The assimilation leads to large corrections on a2 and cc4 during that short period.

5. CONCLUSIONS

The combined state-parameter estimation in a 3-D coupled physical-ecosystem model of the North Atlantic leads to mixed results. We noted a significant reduction of the forecast error in areas continuously observed, notably in winter. As expected, the assimilation is able to correct the parameters according to the local bias and gap to the observations. Nevertheless, the assimilation system reached a lot of difficulties due to a strong model bias. Accurate 8 days forecast could not be produced during the spring bloom. Several parameters converged locally towards unlikely values pointing out potential misrepresentations of the error from the ensemble. Finally, the absence of satellite observations in the Northern part of the domain (North Sea, Arctic) during the cold period (October to March) is a crucial issue that might compromise the reduction of biases induced from irrelevant parameters. The results are sensitive to the setup of the assimilation, for example the efficiency could have been improved by fine-tuning the localization parameters, but we expect qualitatively similar results. The tails of the anamorphosis are also a sensitive point, so further efforts will evaluate dynamically adaptive anamorphosis functions.

ACKNOWLEDGMENTS

This study has been funded by the eVITA-EnKF project from the Research Council of Norway and the MyOcean IP from the European Commission's 7th FP. A grant of CPU time from the Norwegian Supercomputing Project (NOTUR) has been used.

REFERENCES

- [1] Aksnes D., Ulvestad K., Baliño B., Berntsen J. and Svendsen E., 1995, *Ophelia*, 41, 5-36.
- [2] Bentsen M., Evensen G., Drange H. and Jenkins A.D., 1999, *Monthly Weather Review*, 127, 2733-2740.
- [3] Bertino L., Evensen G. and Wackernagel H., 2003, *International Statistical Reviews*, 71, 223-241.
- [4] Bertino L. and Lisæter K.A., 2008, *Journal of Operational Oceanography*, 1, 2, 15-19.
- [5] Bleck R., 2002, *Ocean Modelling*, 4, 55-88.
- [6] Drange H. and Simonsen K., 1996, NERSC Report 125, Nansen Environmental and Remote Sensing Center, Norway.
- [7] Evensen G., 2003, *Ocean Dynamics*, 53, 343-367.
- [8] Evensen G., 2006, Springer.
- [9] Evensen G., 2009, *IEEE Control Systems Magazine*, 29 (3), 83-104.
- [10] GlobColour Product User Guide, 2010, http://www.globcolour.info/CDR_Docs/GlobCOLOUR_PUG.pdf.
- [11] Gregg W.W. and Casey N.W., 2004, *Remote Sensing of Environment*, 93, 463-479.
- [12] Hansen C., Samuelsen A., 2009, *Journal of Marine Systems*, 75, 1-2, 236-244.
- [13] Hunke E. and Dukowicz J., 1999, *Journal of Geophysical Research*, 27, 1849-1867.
- [14] Johannessen, J.A., Hackett B., Svendsen E., Sjøiland H., Røed L.P., Winther N., Albretsen J., Danielsen D., Pettersson L., M. Skogen and Bertino L., 2007, In *The Norwegian Coastal Current – oceanography and climate*. Edited by R. Stre. Tapir academic press, Trondheim, Norway.
- [15] Losa S.N., Vézina A., Wright D., Lu Y., Thompson K., Dowd M., 2006, *Journal of Marine Systems*, 61, 230-245.
- [16] Natvik L. J. and Evensen G., 2003, *Journal of Marine Systems*, 40-41, 127-153.
- [17] Simon E., Bertino L., 2009, *Ocean Science*, 5, 495-515.
- [18] Skogen M. and Sjøiland H., 1998, *Technical Report Fisken og Havet 18*, Institute of Marine Research, Norway.

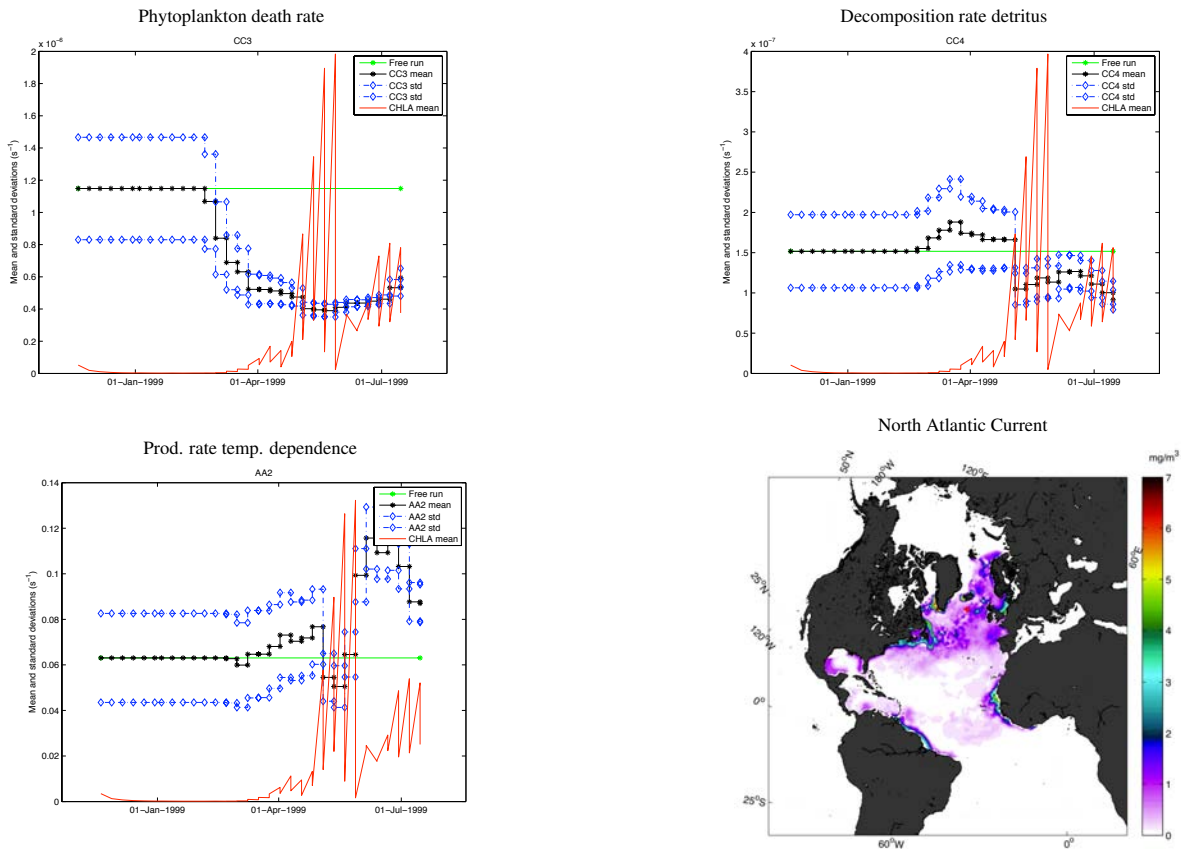


Figure 5. Evolution of local parameters in the North Sea. The grid point is localized with a red cross. The black line represents the evolution of the mean of the ensemble parameter. The blue lines represent the evolution of the mean plus/minus the standard deviation. The green line represents the original value of parameters in NORWECOM. The red curve represents the evolution of chlorophyll-a with time.